ACOUSTIC FIELD STRUCTURE VISUALISATION IN QUASI-COLLINEAR ACOUSTO-OPTIC CELL

Ekaterina Kostyleva[1], Sergey Mantsevich[1]

[1] *Department of Physics, M.V. Lomonosov Moscow State University, Russia*

This paper is a revised version of the authors' submitted manuscript that was peer-reviewed by at least two anonymous reviewers.

Abstract

Some applications of quasi-collinear acousto-optic (AO) cells, such as laser pulse generation and shaping, microscopy, spectroscopy, and multicoloured optical tweezers, require the creation of precisely defined distribution of the acoustic field frequency and amplitude along the entire AO interaction length. If the actual acoustic field structure inside the AO crystal deviates from the desired one, the spectral components of the input optical pulse are diffracted in the areas with improper characteristics. It leads to a distortion of the diffracted beam spectral profile at the output. Numerical modeling is sometimes insufficient, since the AO cells geometry may differ due to an inaccurate fabrication, which significantly modifies the acoustic beam structure along the AO interaction length. In this work, an acoustic field visualization technique for the quasi-collinear geometry of AO interaction is demonstrated as an effective tool for analyzing the redistribution of acoustic power caused by acoustic anisotropy, acoustic power absorption and temperature gradients. We experimentally obtained high-contrast 3D maps of the acoustic power distribution in a quasi-collinear AO cell based on a tellurium dioxide crystal. The proposed approach provides a more consistent and reliable way to characterize the acoustic field structure.

Keywords: *acousto-optics, acoustic field visualization, quasi-collinear interaction, tellurium dioxide, transmission function*

1. Introduction

Quasi-collinear geometry of acousto-optic (AO) diffraction is known for providing abnormally large AO interaction length. As a result, it enables to achieve high spectral resolution in quasi-collinear AO tunable filters and to implement multifrequency diffraction regime which is essential for femtosecond laser pulse generation and shaping and other applications of quasi-collinear AO devices in modern optoelectronics [1], [2], [3], [4]. Due to the extended AO interaction region, the transmission function of a quasi-collinear AO cell is governed by the acoustic power distribution along the entire optical beam propagation path inside the crystal [5]. In the multifrequency diffraction regime applied for femtosecond laser pulse shaping, the acoustic field is a superposition of acoustic waves of different frequencies, each responsible for diffraction of a particular spectral component of the optical pulse in a specific region of the AO crystal [2], [3]. Precise control of the shaped pulse spectrum therefore requires knowledge of the actual power distribution along the AO interaction length for each acoustic frequency component.

However, several physical factors cause the real acoustic field distribution to deviate from the designed one. The strong acoustic anisotropy of paratellurite, especially in the plane orthogonal to the $(1\bar{1}0)$ crystallographic plane, leads to significant redistribution of acoustic power across the beam cross-section and along the AO interaction length [6]. Ultrasound attenuation in the crystal further reduces the acoustic power with propagation distance, while temperature gradients induced by high acoustic power absorption not only modify the AO phase matching conditions [7] but also affect the acoustic wave reflection condition and cause tilting of the reflected acoustic beam[8]. In addition, the finite bandwidth of the AO cell electrical matching circuit may alter the spectrum of short acoustic pulses, leading to a mismatch between the RF drive signal and the acoustic field actually formed inside the crystal.

Since numerical modeling alone cannot fully account for the combined influence of all these factors together with taking into consideration unavoidable fabrication imperfections of the AO device, direct experimental visualization of the acoustic field structure becomes an indispensable diagnostic tool [9]. In this work, we present an acoustic field visualization technique for the quasi-collinear geometry of AO interaction and apply

Corresponding author: *kostyleva.ei16@physics.msu.ru.*

it to a TeO_2-based AO cell to visualise the acoustic power redistribution of 51.5 MHz acoustic wave and to calculate the acoustic attenuation coefficient using the obtained experimental data. We discuss the influence of electrical matching bandwidth on the acoustic pulse spectrum, analyze the acoustic power redistribution due to crystal anisotropy, and study acoustic power absorption, establishing how each factor affects the acoustic field structure in the AO interaction region.

2. Acoustic field visualization

2.1. Experimental technique

The examined AO cell is schematically shown in Fig. 1. The slow shear acoustic mode propagates in the $(1\bar{1}0)$ plane of the TeO_2 crystal, with the phase velocity of the reflected acoustic wave $\mathbf{V}_{ph1}$ directed at 1.8° to the [110] axis. The figure presents a cross-section of the cell in the $(1\bar{1}0)$ plane. The plane orthogonal to $(1\bar{1}0)$ is perpendicular to the figure plane. The incident (2) and reflected (1) acoustic beams are characterised by their group velocity vectors $\mathbf{V}_{g2}$ and $\mathbf{V}_{g1}$, respectively. The acoustic energy walk-off angles of the incident (2) and reflected (1) acoustic beams are marked as ψ_2 and ψ_1. The angle between the piezoelectric transducer facet and the acoustic reflecting facet of the AO cell is denoted Θ. The incident and diffracted optical beams, with wave vectors $\mathbf{k}_i$ and $\mathbf{k}_d$, are shown by red arrows.

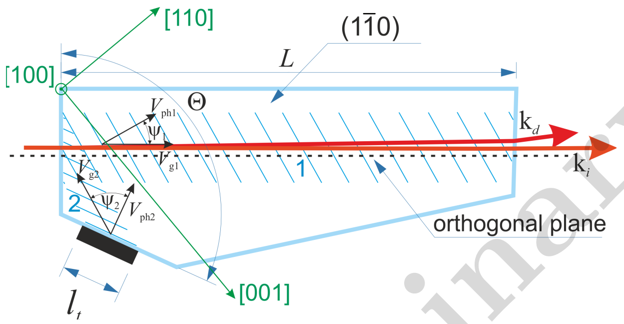

Figure 1: Schematic cross-section of the examined quasi-collinear AO cell in the $(1\bar{1}0)$ plane.

The acoustic field visualization method is based on the time-resolved AO visualization: the distribution of ultrasound power in the region of AO interaction in quasi-collinear AO cell is determined from the diffracted light intensity time dependence. The physical basis of this technique is the following.

In the low-efficiency Bragg diffraction regime, the diffracted optical beam intensity I_d is proportional to the acoustic power P_a in the area of AO interaction:

$$I_d\left(l\right) = I_i\left(\frac{ql}{2}\right)^2 = I_i\frac{MlP_a}{4b}, \qquad (1)$$

where I_i is the incident optical beam intensity, l is the AO interaction length, q is the AO coupling coefficient, M is the AO figure of merit, P_a is the acoustic power value, and b is the acoustic beam width.

Thus, the ultrasound wave power value in the AO interaction region can be directly determined by measuring the diffracted optical beam intensity in different geometries of AO diffraction [10].

But the longitudinal redistribution of acoustic power along the AO interaction length can be obtained in case of collinearity of acoustic and optical input beam by using short acoustic pulses with duration τ_p much shorter than the acoustic wave propagation time along the entire AO cell length applied to the piezoelectric transducer [11]:

$$\tau_p \ll \frac{L}{V_g}, \qquad (2)$$

where L is the AO cell length and V_g is the acoustic group velocity. Under this condition, at any given moment only a spatially localized region of the crystal contains the acoustic pulse, and the AO interaction occurs only in this region.

To record the acoustic field distribution, a continuous-wave input optical beam is directed onto the input optical facet of the AO cell. As the acoustic pulse propagates through the crystal, the diffracted optical beam intensity is registered by the photodetector and observed with oscilloscope. The time-dependence of the diffracted light intensity can be recalculated into a spatial coordinate along the AO interaction length because the acoustic group velocity V_g value is known. The resulting spatial profile represents the acoustic power distribution at the scanned optical beam position.

It should be noted that the choice of the optical beam diameter significantly affects the measurement results. For a narrow beam, the measured power distribution reflects both acoustic attenuation and anisotropy-induced power redistribution. A wider beam provides averaging over a larger area, reducing the influence of local inhomogeneities and yielding a more reliable estimate of the attenuation coefficient [11].

Full three-dimensional mapping of the acoustic power distribution inside the quasi-collinear AO cell is achieved by scanning the optical beam over the input optical facet of the AO cell. For each position, the oscilloscope trace is recorded and processed independently, yielding a complete three-dimensional dataset characterizing the acoustic field amplitude distribution throughout the entire volume of the AO crystal.

2.2. Acoustic pulse duration and electrical matching bandwidth

The spatial resolution of the acoustic field visualization is determined by the acoustic pulse length inside the crystal: $V_g \cdot \tau_p$. To visualise the inhomogeneities of the acoustic beam structure, for example, near the reflecting facet of the AO cell, with characteristic spatial scale of the inhomogeneities $d = 0.5$ mm, a pulse duration of $\tau_p \leq d/2V_g$ is required.

However, the frequency spectrum of the shorter acoustic pulse is wider and it may exceed the bandwidth of the AO cell electrical matching circuit. As a result, the acoustic beam shape inside the crystal may differ

significantly from the designed one, which undermines the reliability of the visualization results.
Therefore, prior to selecting the pulse duration, the standing wave ratio (SWR) of the AO cell over the frequency range should be taken into consideration. If the SWR variation within the frequency range of the acoustic pulse spectrum is small and the matching circuit does not significantly distort the pulse spectrum, the measured diffracted light intensity represents the real acoustic power distribution inside the crystal.
The SWR of the examined AO cell was obtained in the frequency range of interest using a network analyser. To estimate the acoustic pulse spectrum inside the crystal, the spectrum of the RF drive signal at the input of the matching circuit was multiplied by the frequency-dependent power transmission coefficient derived from the measured SWR. The comparison of the resulting simulated acoustic spectrum with the input RF spectrum confirmed that for the pulse durations varied between 0.5 and 4 μs, the matching bandwidth of the examined AO cell does not affect the acoustic pulse form significantly confirming the applicability of the visualization technique.
In our experiment,decreasing the pulse duration improved the spatial resolution in the near-field, whereas in the far-field the images obtained for different pulse durations are nearly identical due to the absence of fine structure at those distances.

3. Acoustic power redistribution

Two main factors cause the acoustic power redistribution inside the quasi-collinear AO cell: ultrasound attenuation in the paratellurite crystal and the acoustic anisotropy, which is especially strong in the plane orthogonal to the $(1\bar{1}0)$ crystallographic plane [12].
The acoustic anisotropy of TeO_2 is characterised by two coefficients, κ_ϕ and κ_θ, which quantify the angular spreading of the acoustic beam energy in the plane orthogonal to $(1\bar{1}0)$ and in the $(1\bar{1}0)$ plane, respectively. Fig. 2 shows the dependence of both coefficients on the angle α between the acoustic wave phase velocity vector and the [110] axis in the $(1\bar{1}0)$ plane.

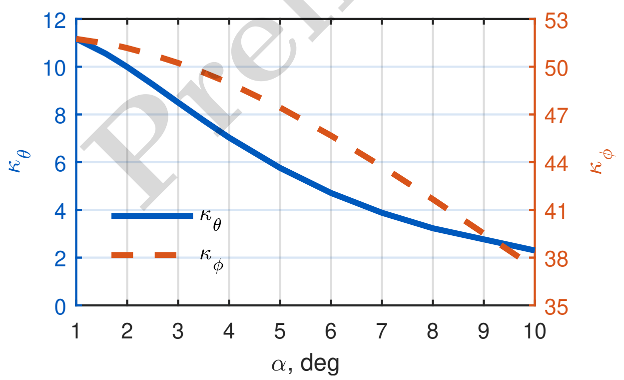

Figure 2: Acoustic anisotropy coefficients κ_θ and κ_ϕ of TeO_2 crystal dependence on the angle α between the acoustic wave phase velocity vector and the [110] axis in the $(1\bar{1}0)$ plane.

The anisotropy coefficient κ_ϕ in $(1\bar{1}0)$ plane reaches a value of about 51.2 for the examined AO cell. High κ_ϕ value leads to spatial redistribution of acoustic power across the beam cross-section at small distances from the reflecting facet.
Fig. 3 shows the acoustic field power distribution in the plane orthogonal to $(1\bar{1}0)$, obtained at 1.55 μm for ultrasound frequency 51.5 MHz with an acoustic pulse duration of 1 μs. Due to the high acoustic anisotropy in this plane, the far-field diffraction zone is observed at a distance of approximately 15 mm from the reflecting facet. Fine-scale inhomogeneities with dimensions below 0.5 mm are clearly resolved in the near-field region within 25 mm from the reflecting facet.

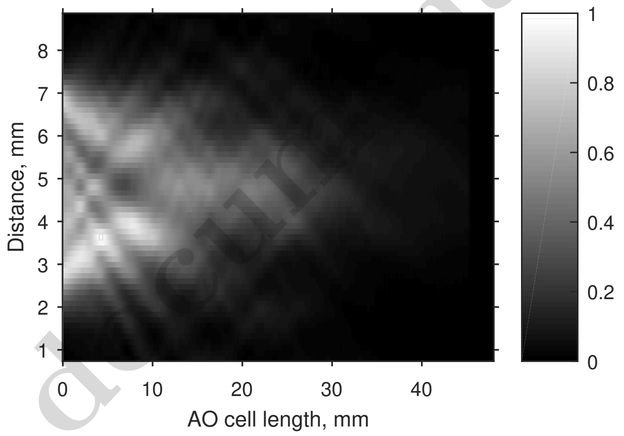

Figure 3: Acoustic power redistribution in AO cell at 5 mm from the facet containing the piezoelectric transducer in the plane orthogonal to $(1\bar{1}0)$.

Fig. 4 presents the acoustic field amplitude distribution in the $(1\bar{1}0)$ plane at a distance of 5 mm from the bottom facet under the same ultrasound frequency and pulse duration.

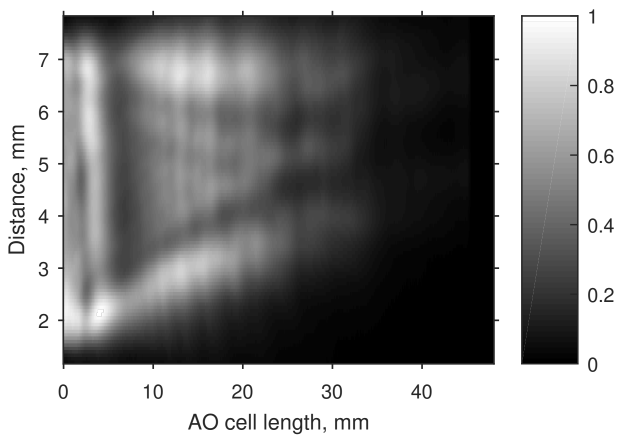

Figure 4: Acoustic power redistribution in AO cell at 5 mm from the bottom facet in the $(1\bar{1}0)$ plane.

For the same AO cell the κ_θ value is five times smaller. This is why the acoustic beam structure in the $(1\bar{1}0)$

plane remains much more homogeneous over a longer distance and the transition to the far-field diffraction regime is shifted far from the reflecting facet of the AO cell, which is clearly seen in Fig. 4.

Although the resulting pattern appears less inhomogeneous than in the orthogonal plane, it is equally important for a complete three-dimensional characterization of the acoustic field, since the knowledge of the acoustic power redistribution in the whole volume of the AO cell is crucial to correctly design the driving acoustic signal and to exploit the quasi-collinear AO diffraction for femtosecond laser pulse shaping. To reconstruct the acoustic power redistribution inside the whole volume of AO interaction we have obtained more than 50 visualisations as in Fig. 3 and Fig. 4.

In addition to the analysis of acoustic power redistribution in different planes due to acoustic anisotropy, the three-dimensional acoustic field map can be used to determine the effective ultrasound attenuation coefficient along the AO interaction length for chosen acoustic signal frequency. For that purpose for each coordinate along the AO interaction length z the measured acoustic power was integrated over the entire transverse plane, yielding the total acoustic power transmitted through the corresponding cross-section of the AO cell as a function of the longitudinal coordinate x. The obtained dependence $P(x)$ can be then approximated by an exponential function.

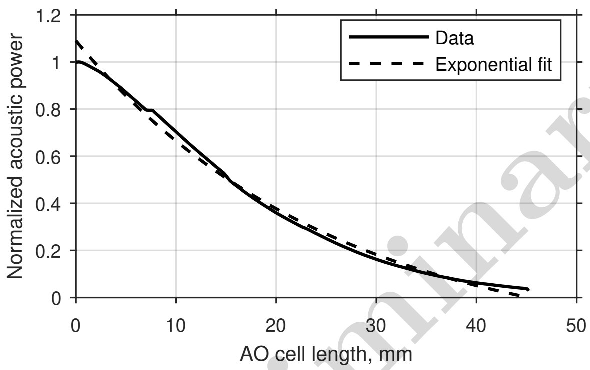

Figure 5: Acoustic power in the AO cell cross-section value dependence on the distance from the reflecting facet and its exponential fit for ultrasound frequency 51.5 MHz.

For the examined quasi-collinear AO cell with acoustic wave propagation direction after reflection 1.8° to the [110] axis in $(1\bar{1}0)$ plane the acoustic power attenuation coefficient for 51.5 MHz was obtained: $\gamma = 0.39$ cm^{-1} or 1.7 dB/cm.

These values can be compared with the attenuation coefficients obtained earlier using the AO method. For the slow shear acoustic wave propagating at an angle of 1.58° to the [110] axis in the (110) plane, the attenuation coefficient increases linearly with ultrasound frequency from $\gamma = 0.39$ cm^{-1} at 87 MHz to $\gamma = 1.43$ cm^{-1} at 176 MHz [11]. Thus, the effective value $\gamma \approx 0.40$ cm^{-1} obtained from the three-dimensional field map for 51.5 MHz is close to the attenuation coefficients obtained for quasi-collinear AO cell with acoustic wave propagation direction closer to [110] axis in $(1\bar{1}0)$ at 87 MHz.

4. Conclusions

An acoustic field visualization technique for the quasi-collinear geometry of AO interaction has been demonstrated and applied to a TeO_2-based AO cell. The implied method relies on time-resolved detection of the diffracted optical beam intensity produced by short acoustic pulses scanned across the input optical facet of the crystal, yielding high-contrast three-dimensional maps of the acoustic power distribution throughout the entire volume of AO interaction.

Prior to performing the measurements, the SWR of the AO cell was analyzed over the relevant frequency range, confirming that the electrical matching bandwidth does not significantly distort the acoustic pulse spectrum.

The obtained acoustic field maps reveal the combined influence of the factors governing the acoustic power redistribution: strong acoustic anisotropy of paratellurite, ultrasound attenuation. In particular, the high acoustic anisotropy coefficient $\kappa_\phi \approx 51.2$ in the plane orthogonal to $(1\bar{1}0)$ leads to a significant inhomogeneity in acoustic power distribution over AO cell volume, whereas the acoustic beam structure in the $(1\bar{1}0)$ plane remains more homogeneous over longer propagation distances. The effective acoustic power attenuation coefficient at 51.5 MHz was determined from the three-dimensional field map as $\gamma = 0.39$ cm^{-1} (1.7 dB/cm), which is consistent with previously reported values obtained by the AO method for close acoustic wave propagation direction.

The proposed technique provides a consistent and reliable experimental tool for discovering the acoustic field structure in quasi-collinear AO cells. Knowledge of the actual three-dimensional acoustic power distribution is directly relevant to the practical design of driving RF signals for implementation of multifrequency AO diffraction regime, and is indispensable tool for femtosecond laser pulse shaping applications, where precise control of the acoustic amplitude at each frequency component along the AO interaction length is required. The approach can serve as a diagnostic method for fabricated AO devices.

5. Acknowledgments

E.I. Kostyleva expresses her gratitude for the personal support to the Theoretical Physics and Mathematics Advancement Foundation “BASIS” (grant 22-2-10-5-1).

References

[1] J. Sapriel, D. Charissoux, V. Voloshinov, and V. Molchanov, “Tunable acoustooptic filters and equalizers for WDM applications,” *Journal of Lightwave Technology*, vol. 20, no. 5, pp. 892–899, May 2002.

[2] F. Verluise, V. Laude, J.-p. Huignard, P. Tournois, and A. Migus, "Arbitrary dispersion control of ultrashort optical pulses with acoustic waves," *Journal of the Optical Society of America B*, vol. 17, no. 1, p. 138, Jan. 2000.

[3] A. M. Weiner, "Ultrafast optical pulse shaping: A tutorial review," *Optics Communications*, vol. 284, no. 15, pp. 3669–3692, 2011.

[4] D. V. Obydennov, K. B. Yushkov, and V. Y. Molchanov, "Independent multicolored bottle-beam generation using acousto-optic spatial shaping of a femtosecond laser beam," *Optics Letters*, vol. 48, no. 20, p. 5320, Oct. 2023.

[5] K. B. Yushkov, A. I. Chizhikov, O. Y. Makarov, and V. Y. Molchanov, "Optimization of noncollinear AOTF design for laser beam shaping," *Applied Optics*, vol. 59, no. 28, p. 8575, Oct. 2020.

[6] S. N. Mantsevich and K. B. Yushkov, "Optimization of piezotransducer dimensions for quasicollinear paratellurite AOTF," *Ultrasonics*, vol. 112, no. November 2020, p. 106 335, 2021.

[7] S. Mantsevich and E. Kostyleva, "Examination of the temperature influence on phase matching frequency in tunable acousto-optic filters," *Ultrasonics*, vol. 91, no. January 2019, pp. 45–51, Jan. 2019.

[8] S. N. Mantsevich, E. I. Kostyleva, K. B. Yushkov, and V. Y. Molchanov, "Experimental observation of reflected acoustic beam tilting with temperature in quasi-collinear acousto-optic filters," *Applied Acoustics*, vol. 233, no. February, p. 110 632, 2025.

[9] E. I. Kostyleva and S. N. Mantsevich, "Acoustic Field Structure Study in Tellurium Dioxide Quasi-Collinear Acousto-Optic Cells," in *2024 Wave Electronics and its Application in Information and Telecommunication Systems (WECONF)*, IEEE, Jun. 2024, pp. 1–4.

[10] S. Mantsevich and E. Kostyleva, "Shear acoustic wave attenuation influence on acousto-optic diffraction in tellurium dioxide crystal," *Applied Optics*, vol. 59, no. 22, pp. 6796–6802, Aug. 2020.

[11] S. N. Mantsevich and E. I. Kostyleva, "Examination of an acoustic field longitudinal power distribution in quasicollinear acousto-optic cells," *Ultrasonics*, vol. 128, no. June 2022, p. 106 875, Feb. 2023.

[12] S. Mantsevich, V. Molchanov, K. Yushkov, V. Khorkin, and M. Kupreychik, "Acoustic field structure simulation in quasi-collinear acousto-optic cells with ultrasound beam reflection," *Ultrasonics*, vol. 78, pp. 175–184, Jul. 2017.